CYCLIC TESTING OF UNBONDED POST-TENSIONED CONCRETE WALL SYSTEMS WITH AND WITHOUT SUPPLEMENTAL DAMPING

K M Twigden[a], S Sritharan[b], and R S Henry[a]

a – **Corresponding author**: Department of Civil and Environmental Engineering, University of Auckland, Private Bag 92019, Auckland 1142, New Zealand. Email: kimberleytwigden@gmail.com . Ph: +64212504401 (K Twigden). rs.henry@auckland.ac.nz (R S Henry)

b - Department of Civil, Construction, and Environmental Engineering, Iowa State University. Email: sri@iastate.edu

ABSTRACT: A series of cyclic lateral-load tests were conducted on four different unbonded post-tensioned precast concrete wall systems, including two Single Rocking Walls (SRW) and two PREcast Wall with End Columns (PreWEC). The main purpose of these tests was to systematically investigate the cyclic response of post-tensioned concrete walls with varying amounts of supplemental damping while keeping the initial post-tensioning force, wall dimensions, and confinement details constant. A secondary objective was to validate the wall panel design including the appropriate selection of axial force ratio and design of confinement and armouring details. All test walls exhibited excellent performance with uplift and rocking at the wall base with only minor damage observed, consisting of small amounts of spalling in the wall toes. There were consistent observations and measurements of the wall damage, concrete compressive strains, and wall neutral axis depths for both the SRW and PreWEC systems with the same wall panel dimensions. Based on these observations it is concluded that the behaviour of the wall panel in a PreWEC system is independent of the number of energy dissipating O-connectors. The O-connectors increased the hysteretic energy dissipation in the wall system and provided between 1.1-1.4% of additional equivalent viscous damping per connector for the PreWEC walls tested. Overall, the behaviour of the four walls tested confirmed the design procedures used, with both the global force-displacement response and local response parameters predicted with sufficient accuracy using an existing simplified analysis method.

Keywords: Self-centering; Unbonded Post-Tensioning; Precast Concrete; Shear Walls; Cyclic Testing; PreWEC; O-Connector.

1 INTRODUCTION

Structural concrete walls provide strong, stiff, lateral-load resisting elements that can reduce lateral drifts during earthquakes. However, the plastic hinge regions in ductile reinforced concrete walls are subjected to large inelastic strain demands during earthquakes that result in significant structural damage. Recent earthquakes have highlighted the impact of damage caused to ductile reinforced concrete structures, which can result in large economic costs due to business down time, repairs, demolition, and rebuilding [1, 2]. In an effort to control the damage in a structure to a certain performance level and isolate irreparable damage to easily replaceable components, engineers and researchers have developed low-damage seismic resisting systems. Low-damage seismic resisting wall systems can be designed using unbonded post-tensioned (PT) precast concrete panels. Inelastic demand in unbonded PT walls is accommodated through the opening and closing of an existing joint at the wall base, introducing a rocking mechanism. In addition to providing lateral strength to the wall, the unbonded PT tendons are designed to remain elastic during a design-level earthquake to provide a restoring force to minimise residual drifts.

The concept of connecting precast concrete elements together with unbonded PT was introduced during the PREcast Seismic Structural Systems (PRESSS) research program conducted in the 1990's [3]. During the PRESSS program a jointed wall system was developed that consists of two or more PT precast concrete panels connected by energy dissipating connectors. The jointed wall system was included in a five storey prototype building that was tested by Priestley et al. [3]. Following introduction of the PT wall concept, several researchers have investigated simple PT wall systems that consist of a single precast concrete panel with no additional energy dissipating connectors [4-6]. These PT only wall systems uplift and rock at the wall base with no significant material inelasticity and therefore

result in low energy dissipation during cyclic loading. To improve the energy dissipation ability or seismic performance of the unbonded PT concrete walls, additional energy dissipating elements are often used. Researchers have investigated several configurations of unbonded PT concrete wall systems with different energy dissipating elements, such as the previously discussed jointed wall system. An alternative hybrid system was also developed that consists of a single precast concrete wall with a combination of unbonded PT and mild steel reinforcement at the wall-to-foundation interface. A number of researchers have experimentally investigated the hybrid system using either mild steel dissipaters [7-11] and/or viscous dampers [12]. Analytical investigations into hybrid walls with viscous damping, friction damping and hysteretic damping provided using mild steel have been reported [13-15].

Recently a new rocking wall system that consists of a PREcast Wall with End Columns (PreWEC) was developed and experimentally validated [16]. The PreWEC system is a variation on the original jointed wall system, and uses a single precast concrete wall panel with two end columns that are each anchored to the foundation using unbonded PT. The wall is joined to the end columns with specially designed energy dissipating O-connectors developed for the PreWEC system [17]. As with other unbonded PT concrete wall systems, the wall and columns are designed to uplift and rock when a lateral load is applied. The uplift at the wall base results in a relative vertical displacement along the joint between the wall and end columns where the O-connectors are attached. As a result of this vertical displacement, the O-connectors undergo flexural yielding and dissipate seismic energy. The PreWEC system was developed to optimise the moment capacity of the jointed wall system by maximising the lever arm between the PT tendons and the wall compression block. Another

advantage of the system is that the columns undergo relatively small uplift and can therefore be used to support the floor diaphragms and transfer gravity loads.

To better understand the behaviour of PreWEC walls, an experimental study of PT concrete wall systems was conducted. A total of four wall systems were considered, including two single unbonded PT only walls, referred to as Single Rocking Walls (SRW), and two PreWEC systems. The objective of these four wall tests was to systematically investigate the cyclic response of walls with varying amounts of supplemental damping in the form of energy dissipating O-connectors while keeping the initial post-tensioning, wall dimensions and confinement details constant. The wall tests also provided an opportunity to further validate the wall panel design, including the choice of axial force ratio and confinement details, and to compare the experimental results of the walls against an existing simplified analysis method used for the design of PT wall systems.

2 EXPERIMENTAL PROGRAM

The experimental program consisted of pseudo-static cyclic testing of four walls, two SRWs and two PreWEC systems. The specimen dimensions and parameters were selected to represent a target range of typical multi-storey commercial buildings between two to eight stories high in a region with medium to high seismic hazard. The building typology utilised unbonded PT precast concrete walls as the primary lateral force resisting system, and further details of the scale and prototype building are published separately [18]. The design of the test walls followed the New Zealand Concrete Structures Standard (NZS 3101:2006) [19] and used the design method for PT concrete walls proposed by Aaleti and Sritharan [20]. The parameters of SRW-A and SRW-B were varied to investigate the behaviour of two different SRW systems with different geometry and initial post-tensioning force. PreWEC-A and PreWEC-B specimens were designed based on the addition of end columns and energy

dissipating O-connectors to SRW-B. To isolate the influence of the number of O-connectors, all other parameters between SRW-B, PreWEC-A and PreWEC-B systems were kept constant. Two cyclic tests were performed on PreWEC-A which are referred to as PreWEC-A1 and PreWEC-A2.

2.1 Wall specifications

The dimensions, design parameters, and cross section of each test wall are provided in Table 1 and Figure 1. SRW-A and SRW-B consisted of a precast concrete wall panel cast with ducts along the length for placement of the unbonded PT tendons. The wall panel used for SRW-A had a length, thickness and height of 1000 mm, 120 mm and 3000 mm, respectively, while the wall panel used for SRW-B had a length, thickness and height of 800 mm, 125 mm and 2860 mm, respectively. The PT tendons used for SRW-A were 15 mm diameter high strength bars and the PT tendons used for SRW-B, PreWEC-A, and PreWEC-B were 15.2 mm prestressing strand. The targeted initial prestress (fpi) in the wall PT was 239 MPa (0.24fy) for the SRW-A and 696 MPa (0.45fy) for SRW-B, PreWEC-A, and PreWEC-B. The targeted initial prestress force was selected to maximise the wall moment capacity while keeping the axial force ratio (AFR) below 10% to ensure no significant crushing occurred in the wall compression toe [21]. The tendon configuration and initial prestress were designed to ensure that the tendon force did not exceed the yield strength of the strand until lateral drifts over 3% were reached. The measured AFR of each wall, SRW-A, SRW-B, PreWEC-A1, PreWEC-A2, and PreWEC-B were 2.49%, 9.53%, 7.84%, 7.96%, and 8.4% respectively. Where the AFR is defined as the ratio of post-tensioning tendon force plus the wall self-weight and additional weight divided by the axial crushing capacity of the concrete section.

The panels were reinforced with minimum horizontal reinforcement at 100 mm centres, minimum vertical reinforcement with the layout shown in Figure 1, and with specially

designed confinement reinforcement at the wall base spaced at 40 mm centres over a height of 200 mm up the wall, as shown in Figure 2(a) and (b). The confinement reinforcement was designed for the wall toe using the confined concrete model described by Mander et al. [22] with the maximum expected compressive strain in the wall toe calculated using the simplified analysis method proposed by Aaleti and Sritharan [23]. A steel angle base frame constructed from 25×25×5 mm equal angle was cast into each precast wall end for additional confinement and protection of the panel edge, as shown in Figure 2(c).

PreWEC-A and PreWEC-B consisted of identical precast concrete wall panels to SRW-B with the addition of two post-tensioned end columns constructed from concrete filled square steel hollow sections (SHS) with a width, length and thickness of 125×125×5 mm. The targeted initial PT force of the columns was 220 kN per column using a 26 mm diameter stress-bar with an unbonded length of 3000 mm for all PreWEC tests. The targeted initial PT force in the columns was selected using the design procedure published by Aaleti and Sritharan [20]. The O-connectors were placed across the wall-to-column joint, welded to the SHS and steel plates embedded into the precast concrete wall panel.

Appendix B of the New Zealand Concrete Structures Standard (NZS 3101:2006) [19] outlines special provisions for the design of ductile jointed precast concrete structural systems. In an attempt to ensure self-centring, NZS 3101 states that the ratio (λ) of the moment contribution from the restoring forces (PT and axial load) to the energy dissipating elements must be greater than or equal to the overstrength factor for the energy dissipating devices. However, previous research has found that this procedure is inadequate to ensure that self-centring is achieved when realistic PT concrete systems are subjected to earthquake loads [24, 25]. Despite these limitations, λ is still a useful property that represents the relative amount of

energy dissipation in PT systems. The number of O-connectors for PreWEC-A and PreWEC-B were chosen such that the specimen with the higher number of connectors would have a moment contribution from the O-connectors less than but close to that provided by the PT at the design lateral drift. As presented in Table 1, PreWEC-A and PreWEC-B had four and six O-connectors per joint, respectively. For design lateral drifts between 1-2%, the λ ratio for PreWEC-A and PreWEC-B remained approximately constant at 1.8 and 1.25, respectively, which are greater than the minimum value of 1.15 prescribed in Appendix B of NZS 3101:2006.

Table 1 – Wall specifications

Wall Label	Tendon type	f_{pi} (MPa)		f'_c (MPa)	f'_g (MPa)	AFR (f_c/f'_c) (%)		O - Connectors per joint
		Target	Achieved			Target	Achieved	
SRW-A	Bar	239	233	32.0	60.0*	2.0	2.49	-
SRW-B	Strand	696	686	35.0	36.3	7.5	9.53	-
PreWEC-A (1/2)	Strand	696	694/705	42.7	60.2	7.5	7.84/7.96	4
PreWEC-B	Strand	696	710	40.7	48.4	7.5	8.4	6

*grout strength measured one week prior to wall test

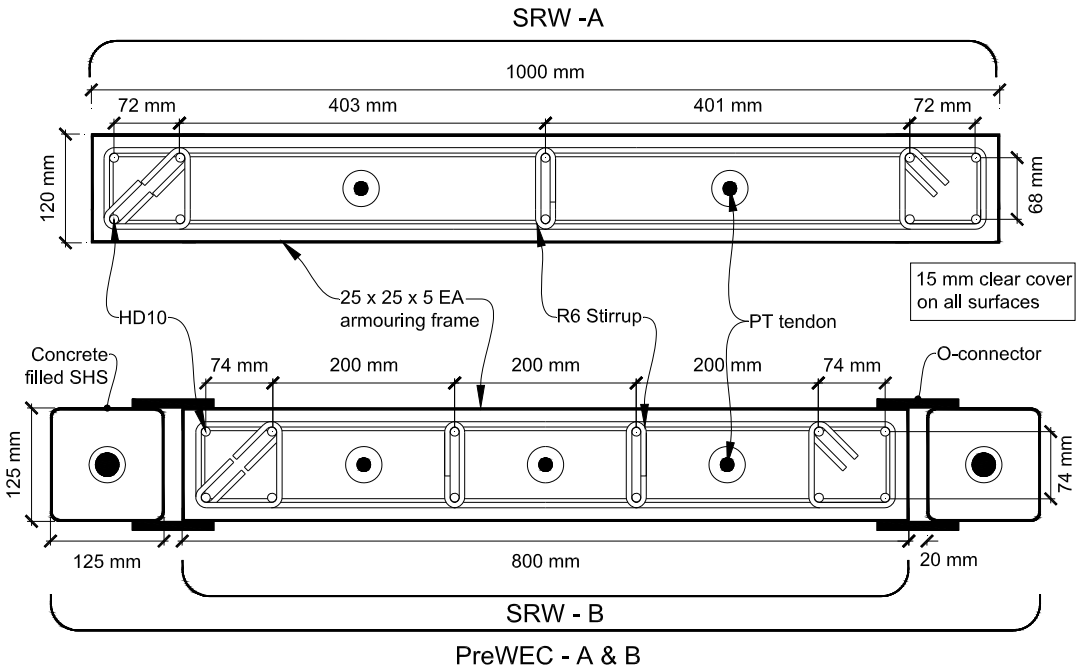

Figure 1 – Wall cross section details

(a) SRW-A

(b) SRW-B and PreWEC-A/B

(c) Armouring angle frame

Figure 2 – Base of wall reinforcement and construction details

2.2 Material properties

In accordance with New Zealand Standards [26], test cylinders and cubes were used to determine the compressive strength of each wall and the grout pad. The measured concrete

(f'_c) and grout (f'_g) strengths on the day of testing for each wall are provided in Table 1. As stated earlier, both 15 mm high strength bar and 15.2 mm strand were used for the wall PT tendon. Three tensile tests per PT tendon were conducted and the measured stress-strain behaviours of the two types of tendon are given in Figure 3(a). All steel tensile testing was conducted in accordance with the metallic materials tensile testing standard [27]. The 15 mm stress bar had an average measured yield stress of 997 MPa, ultimate stress of 1156 MPa, modulus of elasticity of 201 GPa, and cross-sectional area of 177 mm2. The 15.2 mm strand had an average measured yield stress of 1540 MPa, modulus of elasticity of 199.5 GPa, cross-sectional area of 143 mm2 and a measured ultimate stress of 1735 MPa. The ultimate strength was lower than the 1825 MPa stated on the mill test certificate due to premature fracture of strand at the anchorage. Premature fracture of strand at anchorages was found to be a common problem by Walsh and Kurama [28] for monostrand anchorages. In this case the strand failure was not considered critical as the initial prestress was selected to prevent the strand yielding during the cyclic testing. The concrete filled steel tube had an average concrete compressive strength of 38.2 MPa determined on the day of testing of the first PreWEC wall, this value is therefore a minimum for later tests as the same undamaged columns were reused for all tests. The wall vertical and horizontal reinforcement consisted of HD10 (10 mm diameter grade 500 MPa deformed bar) and R6 (6 mm diameter grade 300 MPa round bar) bars respectively. The measured stress-strain response for the reinforcing steel samples are presented in Figure 3(b), including HD10#1 the vertical reinforcement for SRW-A, HD10#2 the vertical reinforcement for SRW-B, PreWEC-A, PreWEC-B, and R6 the horizontal reinforcement for all test walls. The stress-strain response of the HD10 bars showed no significant yield plateau due to the small diameter bars being manufactured from straightened coil stock.

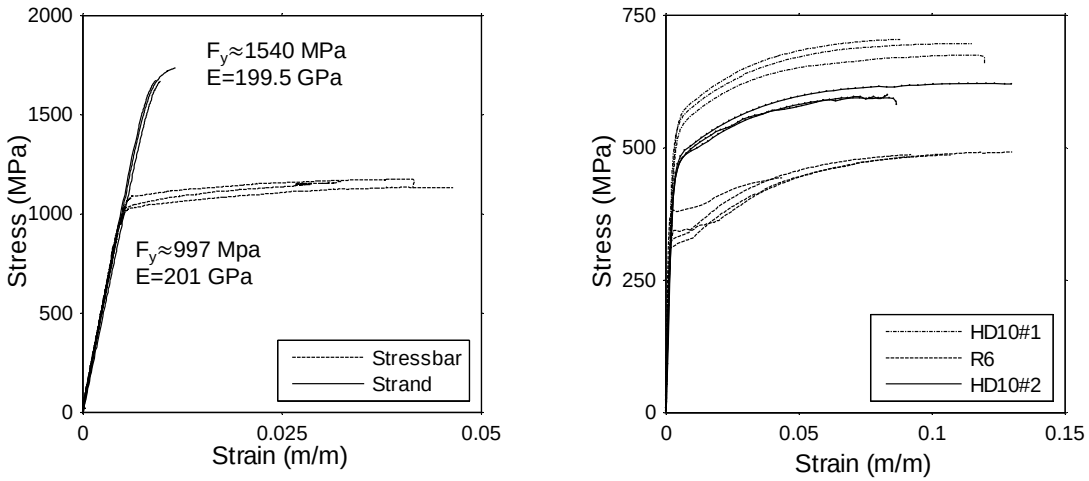

(a) PT tendons (b) Reinforcement

Figure 3 – Measured steel material properties

2.3 O-Connector properties

The O-connector concept was originally developed by Henry et al. [17] and subsequently used during the first PreWEC cyclic test [16]. The O-connectors used for this experimental programme were made from mild steel and designed based on a ½ scale version of the O-connector used by Sritharan et al. [16], except with double the thickness to length ratio to prevent out of plane buckling. The O-connectors were laser cut out of 10 mm thick mild steel plate with the geometry shown in Figure 4(a). The stress-strain behaviour of the mild steel plate established from uniaxial tension tests is shown in Figure 4(b). A component test was performed on the O-connector using the setup shown in Figure 5(a). The test setup consisted of four O-connectors which provided an average connector response. The displacement protocol applied to the O-connectors was identical to the relative vertical displacement of the column to wall measured during the PreWEC-A2 cyclic test. The measured force-displacement response of a single O-connector for the applied relative vertical displacement is shown in Figure 5(b). A stable force-displacement response was observed until fracture of the

O-connectors initiated during the second cycle to 22 mm vertical displacement, which corresponded to 3 % lateral wall drift during the PreWEC-A test.

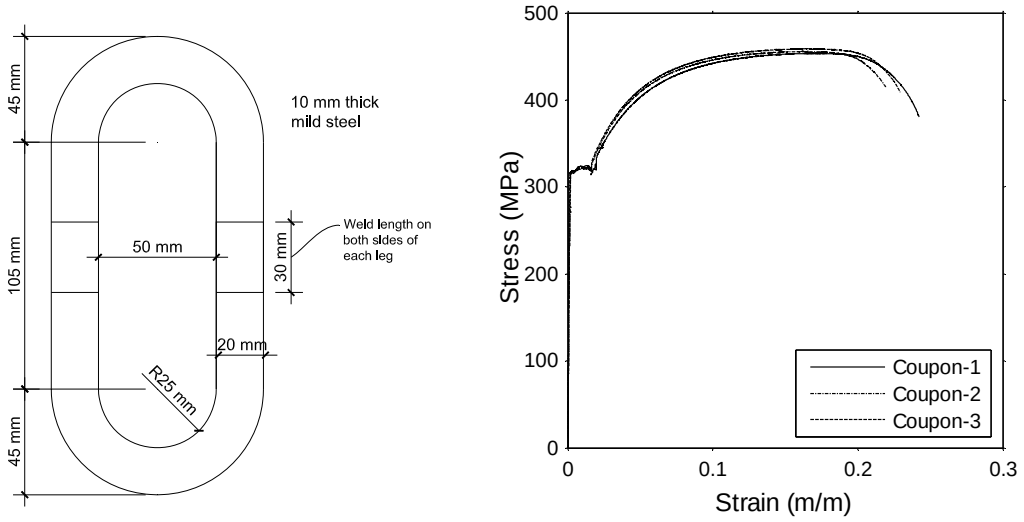

(a) O-connector dimensions (b) Mild steel properties

Figure 4 – O-connector dimensions and steel properties

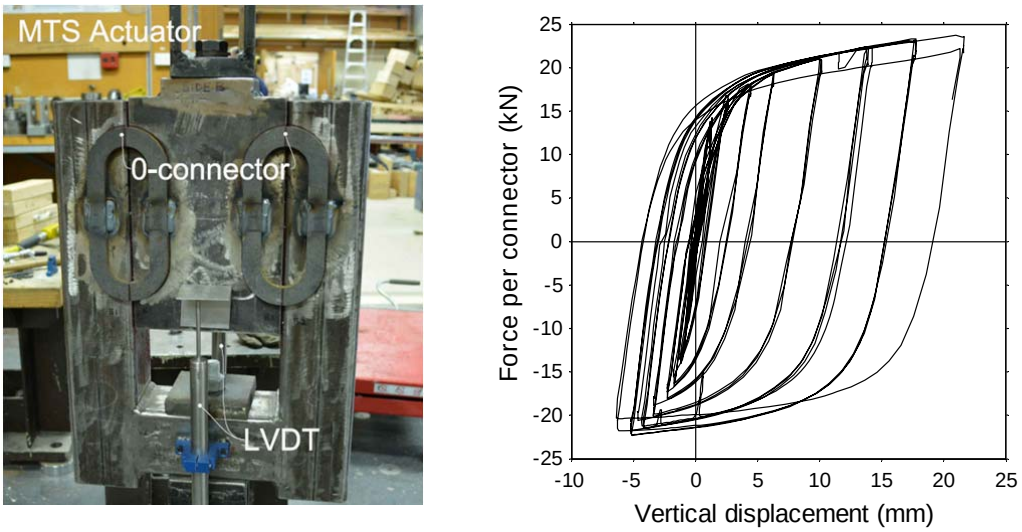

(a) Test setup (b) Force-displacement behaviour

Figure 5 – O-connector test setup and measured response

2.4 Test setup

A schematic and photo of the typical test setup and instrumentation of a PreWEC test is presented in Figure 6. The test setup for the SRW tests was identical except without the columns and O-connectors. The wall panels were erected onto a foundation block that was post-tensioned to the strong floor. A 40 mm deep by 160 mm wide shallow pocket which ran the length of the wall system was provided in the top of the foundation. The wall was initially supported on small 30 mm high shims and high strength grout was flowed under the wall to fill the pocket and provide an even bearing surface at the wall-to-foundation interface. The wall was embedded approximately 10 mm into the grout pocket to increase the sliding shear resistance. To limit the concrete compressive strains and spalling of cover concrete in the toe region, SRW-B, PreWEC-A and PreWEC-B had a foam strip across the width of the cover region (15 mm) glued at each wall end, as depicted in Figure 7(a). It is important to note that use of the foam effectively shortens the length of the wall by 30 mm to 770 mm.

A concrete block was attached and grouted on top of the wall and steel beams were placed adjacent to the block to prevent out-of-plane deformations of the wall. To perform the pseudo-static cyclic testing, a hydraulic actuator was attached through the loading block at a height of 3150 mm for SRW-A and 3 m for SRW-B, PreWEC-A, and PreWEC-B from the wall base. The PT tendons of the walls and columns were anchored between the foundation and top block and remained unbonded over the entire height. The typical unbonded length of wall tendons for SRW-B, PreWEC-A and PreWEC-B was 3600 mm and 3900 mm for SRW-A. The typical strand anchorage is shown in Figure 7(b). A specially designed and manufactured threaded barrel with round nut were used to finely adjust the initial tendon stress and de-stress without having to release the wedges from the barrel. For SRW-B, PreWEC-A and PreWEC-B the top concrete block weighed 31.35 kN and for SRW-A the top concrete block weighed

20.11 kN. The top block provided additional mass for dynamic tests that were performed using the same test setup, but are not reported herein. Due to the slightly different setup between SRW-A and the other test walls SRW-A had a centre of mass, including wall mass, of 2841 mm from the base of the wall while SRW-A, PreWEC-A and PreWEC-B had a centre of mass of 2660 mm from the base of the wall.

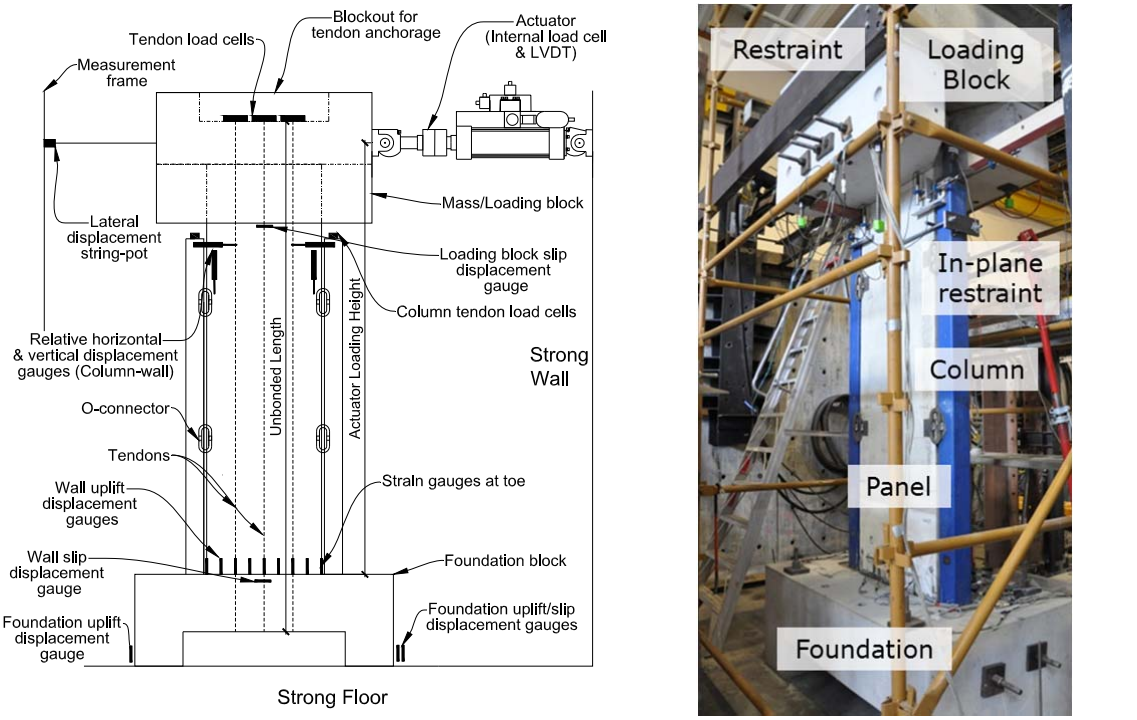

a) Test setup and instrumentation schematic b) Photo of test setup for PreWEC-A

Figure 6 – Test setup and instrumentation schematic for PreWEC tests

2.5 Load protocol

The loading protocol for the test was developed in accordance with ACI guidelines for the acceptance criteria for unbonded PT concrete walls, ACI ITG-5.1 [29]. For SRW-A, PreWEC-A and PreWEC-B, three force based cycles to a maximum of 0.6 times the decompression moment were applied first followed by displacement controlled cycles up to a

maximum of 3% lateral drift, as shown in Figure 8. For SRW-A, a maximum lateral drift of 2% was applied to prevent yielding of the tendons.

a) Wall placement (SRW-B) b) PT anchorage setup

Figure 7 – Wall set up details

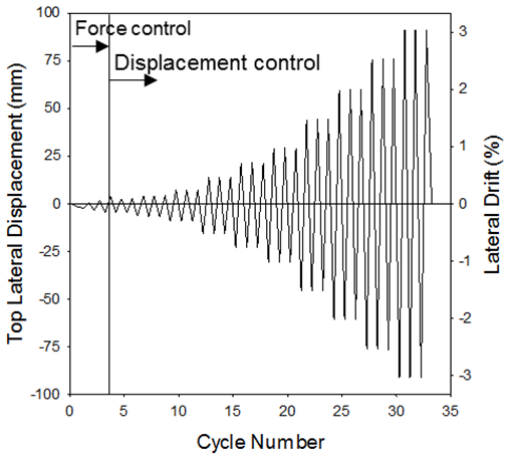

Figure 8 – Typical load protocol

2.6 Instrumentation

The walls were extensively instrumented as depicted in Figure 6(a). Displacement gauges were placed at the base of the wall to measure uplift. Additional displacement gauges were placed at the foundation-floor and wall-loading block interface to monitor slip and unintended uplift of the foundation. A string-pot was used to measure the top lateral displacement at the

actuator height. Load cells were used to measure the lateral load in the actuator as well as the wall and column PT tendon forces. For the PreWEC tests, LVDTs (Linear Variable Differential Transformer) were used to measure the relative vertical and horizontal displacements between the wall and each end column.

Strain gauges were placed both inside and on the surface of the concrete at the wall toe to measure the strain demand. Embedded concrete strain gauges were cast in the confined concrete region of each wall toe for each test. The two embedded gauges for SRW-A had a gauge length of 30 mm and were placed 10 mm in from the wall compression edge, 65 mm up from the wall base and 40 mm from each side. For SRW-B, PreWEC-A1, PreWEC-A2 and PreWEC-B, embedded strain gauges with a 60 mm gauge length were used. For SRW-B the two embedded gauges were placed 10 mm in from the wall compression edge, 25 mm up from the wall base and 42 mm in from each side at each toe. For PreWEC-A and PreWEC-B, the two embedded gauges in each wall toe were placed 30 mm in from the wall compression edge, 35 mm up from the wall base and 45 mm in from each side at each toe. Surface mounted strain gauges were also placed on the end of each wall panel for each test. The SRW-A surface strain gauges were 30 mm long and placed 60 mm up from the wall base and 43 mm in from each side. The surface strain gauges were 60 mm long for SRW-B, PreWEC-A, and PreWEC-B and were placed 60 mm up from the wall base and 35 mm in from each side. All measurements reported are to the centre of the strain gauge.

3 TEST OBSERVATIONS

The four test walls all performed well with uplift occurring at the wall base when compared to the distributed cracking expected from traditional reinforced concrete walls. The typical behaviour of the test walls is shown in Figure 9(a) for PreWEC-B at 3% lateral drift. No flexural cracks were observed in the wall panels and no significant crushing occurred in the

246 compression toe for any of the tests. Only a minor amount of spalling was observed in the
247 wall toes at drifts greater than 2 % and no bending of the steel angle armouring frame used for
248 confinement was observed. Additionally, no slip was observed between the wall and
249 foundation during any of the tests.

250 Although the damage to the wall toes was isolated to a small area and had an insignificant
251 effect on the overall behaviour of the walls, a close up of the toe damage at the end of each
252 test is shown in Figure 10. There is only a small increase in spalling between SRW-A and
253 SRW-B despite SRW-B having almost four times the AFR. The foam strip used in the corner
254 of walls SRW-B, PreWEC-A and PreWEC-B was successful in limiting the spalling of the
255 wall toe, with similar damage observed for all four test walls despite SRW-B, PreWEC-A and
256 PreWEC- B walls having much higher AFR's than SRW-A.

257 The wall and end columns rocked independently during the PreWEC tests and imposed a
258 vertical deformation on the O-connectors at the wall-to-column joint. The deformed shape of
259 one of the O-connectors in PreWEC-B at 3% lateral drift is shown in Figure 9(b). As
260 expected, the O-connector behaviour was dominated by flexural yielding of legs up until
261 failure which occurred during cycles to 3% lateral drift. The displacement capacity and failure
262 mode of the O-connectors was similar to that observed during the component tests discussed
263 earlier. Despite failure of the connectors occurring at 3% lateral drift for most PreWEC tests,
264 it should be noted that the O-connectors can be designed to achieve greater displacement
265 capacity depending on their geometry and steel grade [16, 17].

266 Two cyclic tests were performed on the PreWEC-A wall. The first test (PreWEC-A1) relied
267 solely on the O-connectors to connect the wall to the end columns. During this test it was
268 observed that the columns were pushed and pulled with the wall by the O-connectors causing

horizontal compression and tension to be imposed on the O-connectors. As a result larger than expected horizontal displacements were imposed on the O-connectors resulting in premature failure during the 2.5% lateral drift cycles. Following the first test, the fractured O-connectors were removed and new connectors were welded onto the PreWEC-A wall. An in-plane lateral restraint as shown in Figure 6(b) was added during the second test (PreWEC-A2) to enable the end columns to laterally displace with the wall without relying on the O-connectors. Use of the restraint for PreWEC-A2 resulted in the O-connectors achieving their design displacement, with failure occurring during the 3% lateral drift cycles as expected from the component test. The end column restraints were also used successfully during the PreWEC-B test, with the columns displacing laterally with the wall and O-connector failure again occurring during cycles to 3% lateral drift.

Struts or restraints were also attached between the wall and end columns during the PreWEC test reported by Aaleti et al. [30], but were later found to be not required during the test. In contrast the restraint was required during the tests reported herein due to the relative strengths of the wall, end columns, and O-connectors. A horizontal force of 0.86 kN per O-connector was required to pull the end column to 2% drift during the PreWEC-A test compared to a horizontal force of 0.24 kN per O-connector for the Aaleti et al. PreWEC test. Due to the different connector size, these horizontal forces equated to 3.6% and 0.5% of the O-connector vertical force capacity for the PreWEC-A and Aaleti et al. PreWEC tests respectively. These calculations demonstrate that a seven times greater demand was placed on each O-connector during the PreWEC-A test compared to the Aaleti et al. PreWEC test. Therefore the requirement of the restraints is a function of the relative strengths of the end column and connectors, and should be considered during the design of the O-connectors.

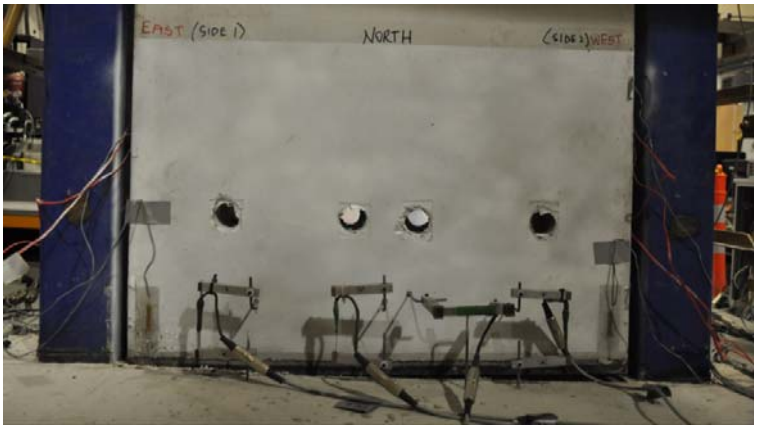

(a) Condition of wall during uplift at 3% drift for PreWEC-B

(b) O-connector at 3% drift for PreWEC-B

Figure 9 – Observed wall behavior

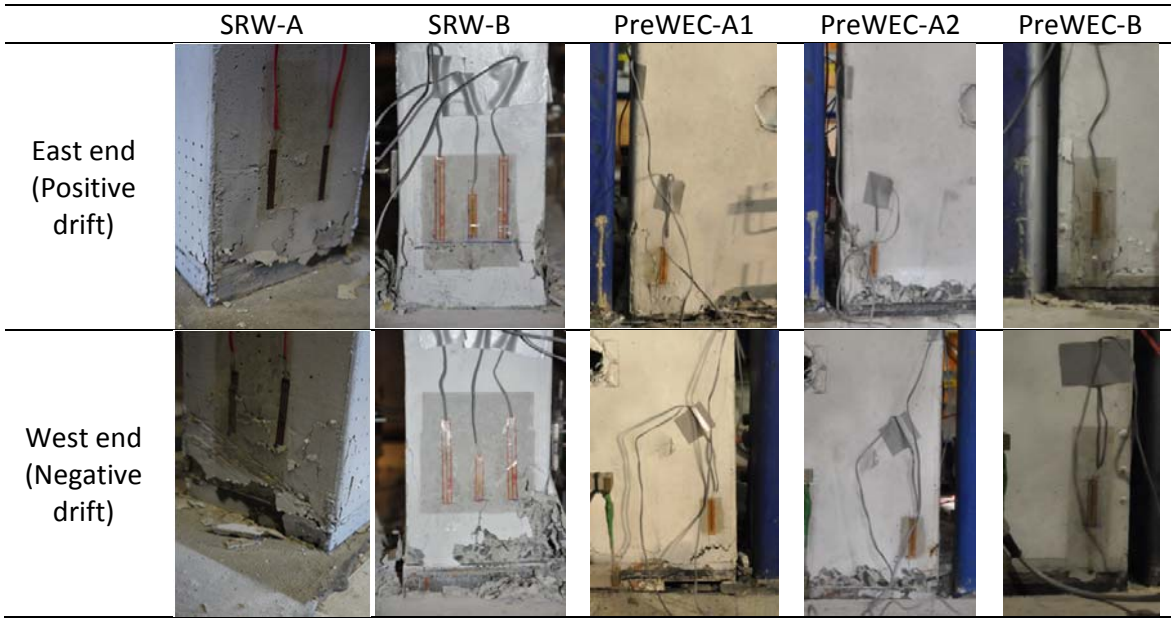

Figure 10 - Observations of wall toe damage for all tests

4 RESULTS AND DISCUSSION

4.1 Force displacement response

The measured lateral force-displacement response for each of the four test walls are shown in Figure 11. The overall behaviour was good with no significant strength degradation until the O-connectors started fracturing during the PreWEC tests, and only minor stiffness

degradation. A simplified analysis approach developed by Aaleti and Sritharan [23] was used to predict the behaviour of the four test walls, and is compared against the measured experimental results in Figure 11. The simplified analysis method accurately captured the envelope of the global behaviour of both the SRW and PreWEC systems.

SRW-A exhibited an imperfect bilinear elastic response with a small amount of hysteresis up until the test finished at 2% lateral drift. SRW-B also exhibited an imperfect bilinear response up until 2% lateral drift at which stage the unloading path altered with increased hysteresis introduced into the system. The change in unloading path could be due to PT loss within the system, debris becoming trapped underneath the wall, or minor inelastic concrete strains in the wall toe.

Both PreWEC-A1 and A2 tests resulted in a similar global force-displacement response with increased hysteresis area when compared to the two SRW tests. A small amount of stiffness softening was observed for PreWEC-A2 when compared to PreWEC-A1 due to the small amount of inelastic concrete strains that occurred in the wall toe during PreWEC-A1. PreWEC-A2 achieved a more desirable force-displacement response in comparison to PreWEC-A1 as the O-connectors fractured during the 3% lateral drift cycles instead of 2.5% lateral drift cycles due to the addition of the end column restraints. As shown in Figure 11(d), PreWEC-B exhibited increased hysteresis area when compared to the SRW tests and the PreWEC-A system due to a 50% increase in the number of connectors. Fracture of the connectors initiated at 3% lateral drift, similar to that observed during the PreWEC-A2 test. The increase in lateral strength and hysteresis from SRW-B to PreWEC-A to PreWEC-B was due to the strength provided by the increasing number of O-connectors, and was accurately predicted by the Aaleti and Sritharan simplified analysis method.

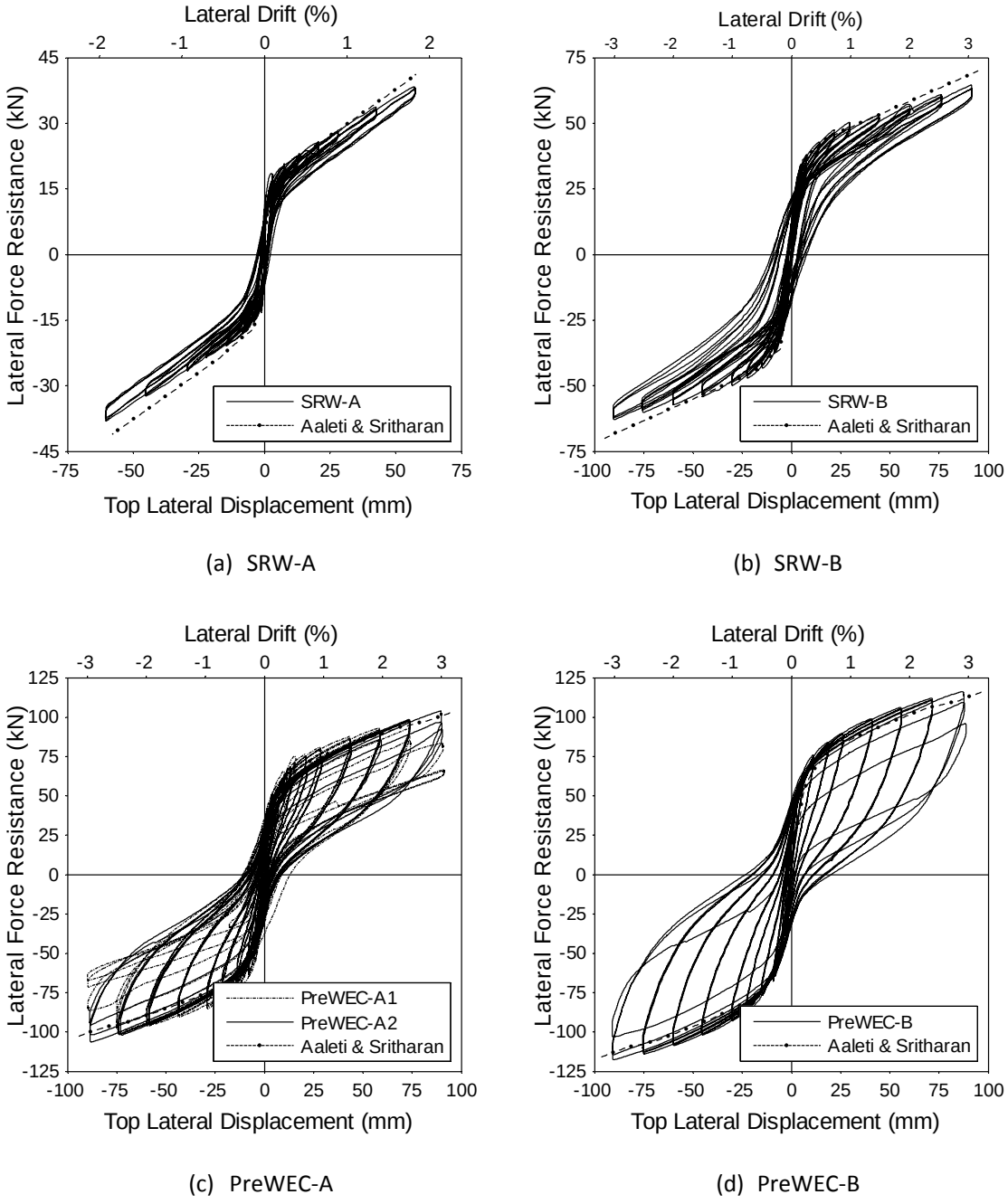

322 **Figure 11 – Measured lateral force-displacement responses for each test**

323 **4.2 Initial stiffness**

324 The stiffness of structural walls is important when calculating the fundamental period of a

325 structure. The initial stiffness of the four test walls was determined from the force based

cycles applied at the start of the loading protocol. A best fit linear trend was used to find the slope (initial stiffness) of the force displacement loading curve for the largest cycle below decompression of each wall system. As presented in Table 2, the measured initial stiffness of SRW-A, SRW-B, PreWEC-A1, PreWEC-A2 and PreWEC-B were 16.36 kN/mm, 8.89 kN/mm, 12.90 kN/mm, 6.34 kN/mm, and 12.19 kN/mm, respectively. During the force based cycles no uplift occurred at the wall base which implies that the expected lateral stiffness should theoretically be calculated based on the gross section moment of inertia (Ig). A prediction of the initial stiffness of each wall is also presented in Table 2, and was calculated assuming a lateral stiffness (k) equal to the sum of 3EIg/h3 for each component (walls and end columns), where E is the modulus of elasticity, I the moment of inertia and h the height of the applied load [31]. The calculation assumed a concrete modulus of elasticity (Ec) equal to $4700\sqrt{f'_c}$, where f'_c is the compressive strength of concrete in MPa. The height used for the column stiffness calculation was the height of load application. The final row in Table 2 is effective stiffness modifier which is the measured initial stiffness divided by the predicted initial stiffness. For all walls use of the gross section properties significantly overestimates the initial stiffness. Despite the two SRW specimens having different section properties they had similar effective stiffness modifier ratios of 0.64 and 0.61 and the two undamaged PreWEC specimens PreWEC-A1 and PreWEC-B had similar effective stiffness modifier ratios of 0.79 and 0.77. The effective stiffness modifier ratio of PreWEC-A2 is not comparable as the wall had already been subjected to the PreWEC-A1 test.

348 **Table 2 – Initial stiffness of each test specimen**

	SRW-A	SRW-B	PreWEC-A1	PreWEC-A2	PreWEC-B
Measured initial stiffness ($K_{i(m)}$) kN/mm	16.36	8.89	12.90	6.34	12.19
Predicted initial stiffness ($K_{i(p)}$) kN/mm	25.52	14.69	16.42	16.42	15.84
Effective stiffness modifier ($K_{i(m)}$/ $K_{i(p)}$))	0.64	0.61	0.79	0.39	0.77

349

350 **4.3 Equivalent viscous damping**

351 Equivalent viscous damping (EVD) is used as a measure of performance as it is essential to
352 displacement based design procedures commonly used for unbonded PT structures. The EVD
353 calculated from the force-displacement hysteresis response for each cycle of the five wall tests
354 is shown in Figure 12(a). Both the SRW specimens had relatively low EVD in comparison to
355 the PreWEC systems due to the lack of energy dissipating O-connectors. The two SRW
356 specimens had a similar amount of EVD up until 1% lateral drift, after which point SRW-B
357 had a slight increase in EVD due to higher compressive strains. SRW-B is expected to have
358 higher compressive strains due to the higher AFR of 9.53% compared to 2.49% for SRW-A.
359 The EVD for the two SRW remained between 3-5% throughout the tests. The difference in
360 EVD between PreWEC-A1 and A2 was attributed to the energy dissipation from
361 irrecoverable inelastic strains that had already been imposed on the wall specimen during the
362 A1 test. The EVD at 2% lateral drift was 4.7%, 15.8%, 14.9% and 17.9% for SRW-B,
363 PreWEC-A1, PreWEC-A2 and PreWEC-B, respectively. The EVD of SRW-B represents the
364 inherent energy dissipation of the PT wall without connectors. Therefore it is reasonable to
365 assume that the EVD difference between SRW-B and the PreWEC systems is equal to the
366 EVD contribution from the O-connectors. For the three PreWEC tests, the EVD per O-
367 connector ranged from 1.1-1.4% at 2% drift.

4.4 Residual drifts

The residual drift is a critical aspect of seismic resilient design and is important to determine if the self-centring objective has been achieved. For the pseudo-static tests the residual drift was defined as the displacement at zero lateral force after unloading from the first peak displacement of each cycle. These calculated residual drifts are plotted for each of the wall tests in Figure 12(b). As expected from the hysteresis response, the residual drifts increased as the lateral drift or supplementary damping increased. From the results for the two SRW systems, it is clear that a higher AFR introduced higher residual drifts due to increased compression strains in the wall toes. For the PreWEC walls the residual drift increased with an increasing number of O-connectors as the hysteresis loops become fatter. However, interesting the residual drift for the PreWEC walls decreased or recovered from 2.5 % to 3 % drift as the connectors started to fracture. It is important to note that the calculated residual drifts from the pseudo-static test results do not account for dynamic response and therefore do not necessarily represent the residual drifts expected following an earthquake due to the "shake-down" effect, such as that reported by Henry et al. [24].

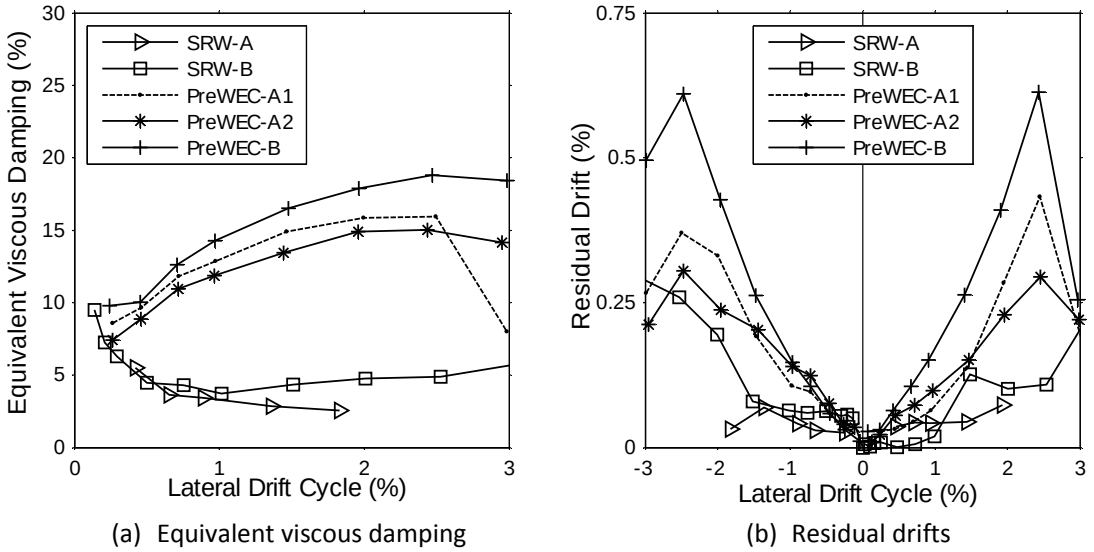

(a) Equivalent viscous damping (b) Residual drifts

Figure 12 – Calculated equivalent viscous damping and residual drift for each test

4.5 Connector behaviour

The relative vertical displacement measured between each end column and the wall at the location of the top O-connectors for the three PreWEC cyclic tests is presented in Figure 13(a). The relative vertical displacement between the wall and end columns reached up to 23 mm at the end with wall uplift and up to 7 mm at the end of with toe compression. By comparing the measured connector displacements from the PreWEC tests to that of the component test shown previously in Figure 5(b), it is proven that the O-connectors yield in both loading directions in the PreWEC system. The relative vertical displacement measured between each end column and the wall was almost identical for all of the PreWEC tests, which implies similar panel behaviour regardless of O-connector number.

Figure 13(b) presents the change in relative horizontal displacement between the wall and east column with lateral drift. Only the east column is presented due to the symmetrical behaviour observed. PreWEC-A1 achieved the highest relative horizontal displacement, up to 6 mm, due to the lack of a restraint between the wall and columns. PreWEC-A2 and PreWEC-B indicate significantly lower relative horizontal displacements due to the addition of the restraint between the wall and columns that limited the horizontal force resisted by the O-connectors. The higher relative horizontal displacement caused the early failure of the O-connectors during the PreWEC-A1 test due to the increased strain demand. The effect of the increased strain demand was successfully eliminated for the PreWEC-A2 and PreWEC-B tests through the addition of the restraints. Evidence of this is shown by the increased performance of the O-connectors failing during the 3 % lateral drift cycle for both PreWEC-A2 and PreWEC-B, and also the purely vertical displacement component test presented earlier in Figure 5(b), which shows failure during the same lateral drift cycle as the PreWEC-A2 wall test.

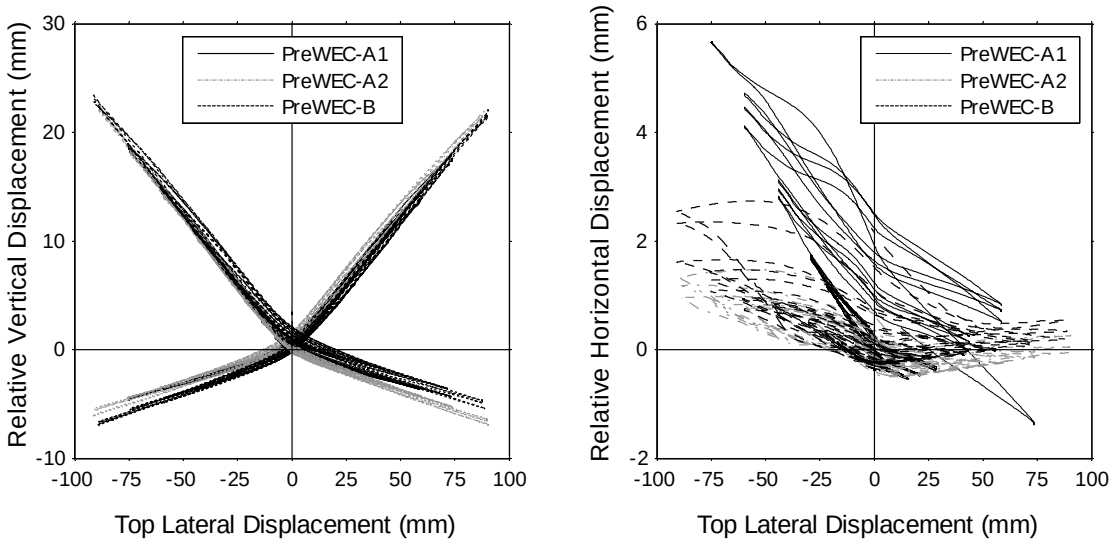

(a) Relative vertical displacement

(b) Relative horizontal displacement east column

Figure 13 – Measured relative vertical and horizontal deformation of the O-connectors

4.6 PT force

The measured change in total wall PT force with lateral drift for the five tests are shown in Figure 14, alongside the predicted PT force from the Aaleti and Sritharan simplified analysis method. As expected, gap opening at the wall base caused the PT force to increase with increasing lateral drift. The overall behaviour of the tendons for all tests was essentially elastic as the PT tendon type and initial prestress were specifically designed to avoid any tendon yielding during up to 3 % lateral drift for SRW-B, PreWEC-A and PreWEC-B and up to 2 % lateral drift for SRW-A.

The prestress losses were minimised by pre-seating the tendon anchorage up to a force equivalent to 0.68fy. Despite pre-seating the tendons and avoiding tendon yielding, prestress losses occurred consistently throughout the tests at the peak of each first drift cycle. The total prestress loss measured for SRW-A, SRW-B, PreWEC-A1, PreWEC-A2, and PreWEC-B was

16.6 %, 7.3 %, 16.2 %, 6.6 %, and 14.4 %, respectively. As a result of these losses, the predicted tendon force was overestimated by the simplified analytical method. The losses were attributed to further wedge draw in at the anchor as the tendon force increased and wall shortening as the compression toes were subjected to inelastic strains. As depicted in Figure 14 (c), PreWEC-A2 underwent less prestress loss compared to PreWEC-A1 as the tendon anchorages had technically been pre-seated further due to the PreWEC-A1 test. PreWEC-A1 and PreWEC-B experienced similar prestress loss throughout each test, this shows a degree of predictability with the amount of prestress loss. If the entire loss was assumed to be due to wedge draw in at the anchor the quantity of draw in based on the total prestress loss and unbonded tendon length would be equal to 2.0 mm for PreWEC-A1 and 1.8 mm for PreWEC-B. However, it is important to note that the wedge draw occurs as a fixed displacement irrespective of tendon length. Therefore, the PT losses observed in the four reported tests are likely to have been amplified due to the reduced wall scale and short tendon length. Significantly less PT loss would be expected when the tendon length is longer in a full-scale PT wall.

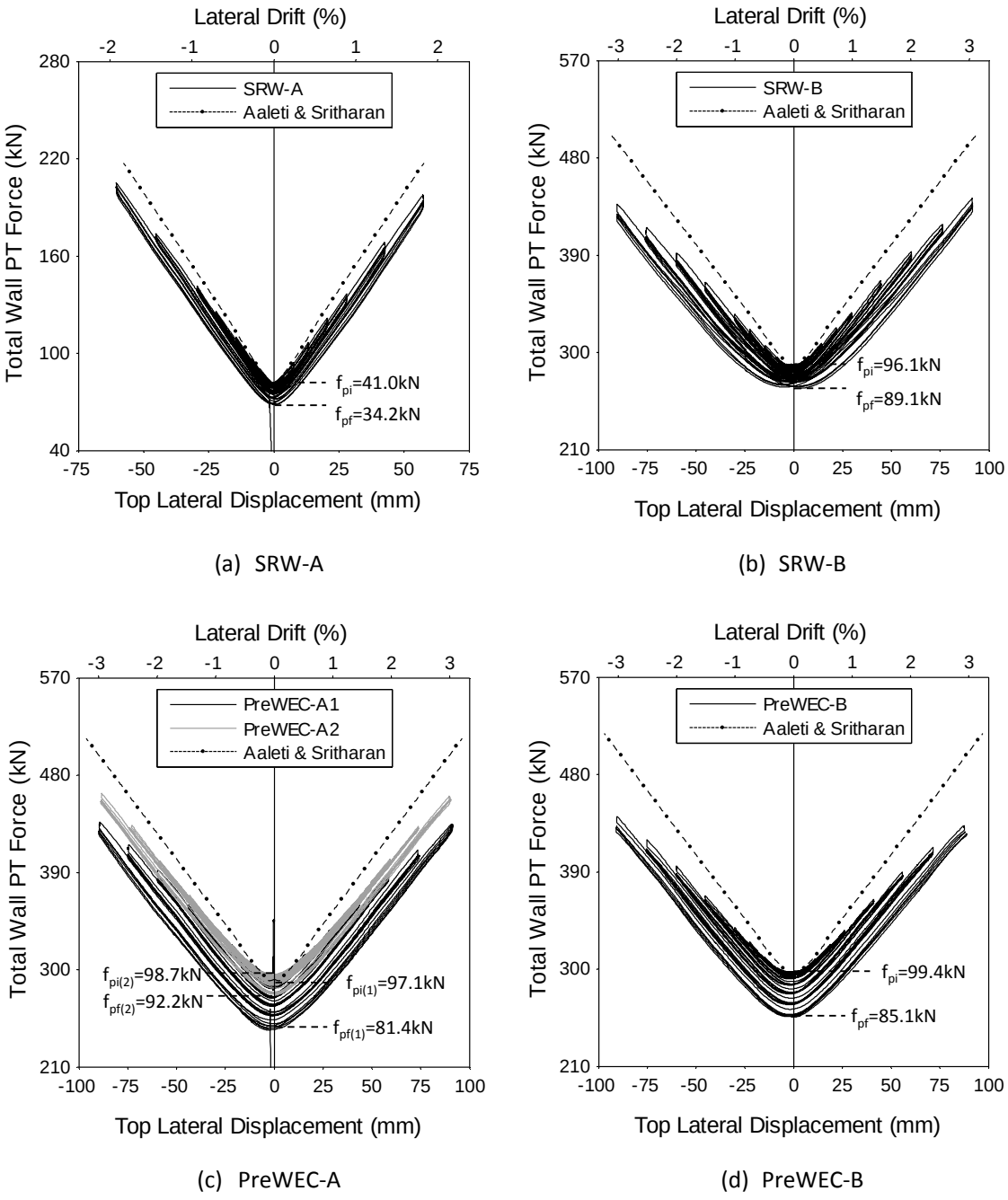

435 **Figure 14 – Measured wall PT force**

436 **4.7 Neutral axis depth**

437 As previously described in section 3, all of the test walls exhibited uplift at the wall base due

438 to rocking. An important parameter to understanding the behaviour of the systems is the

length of wall in contact with the foundation known as the neutral axis (NA) depth. The neutral axis depth of each wall was calculated by fitting a linear function through the measured uplift of the displacement gauges at the wall base. The rotation at the wall base was first calculated and then the neutral axis depth determined from rotation, uplift and the known wall length. The width of foam strip at each wall end of 30 mm total was taken into account when determining the neutral axis depth for SRW-B, PreWEC-A and PreWEC-B by using an effective wall length of 770 mm. Both the measured rotation and NA depth at the peak of each lateral drift cycle are presented for each test in Figure 15. The measured NA was stable between the three cycles with no NA migration for all tests. The stable NA between cycles demonstrates that no significant crushing occurred and that the walls were well designed. As shown by Figure 15(a), (c), (e), and (g), the rotation was well predicted by the simplified analytical method proposed by Aaleti and Sritharan [23] for all tests. The experimental NA at larger lateral drifts correlated well with analytical predictions, but was typically under-predicted for lateral drifts less than 2%, as demonstrated by Figure 15(b), (d), (f), and (h). The average measured neutral axis depths at 3% lateral drift for SRW-B, PreWEC-A and PreWEC-B were 99.3, 82.78, and 103.6 mm, respectively. The relatively similar NA depths demonstrate that the wall behaviour appeared to be independent of the number of O-connectors when considering the differences expected due to the concrete strengths, grout strengths and PT force.

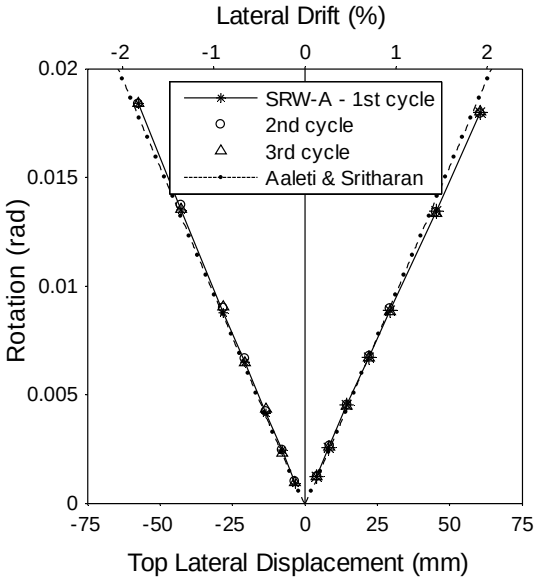

(a) SRW-A rotation

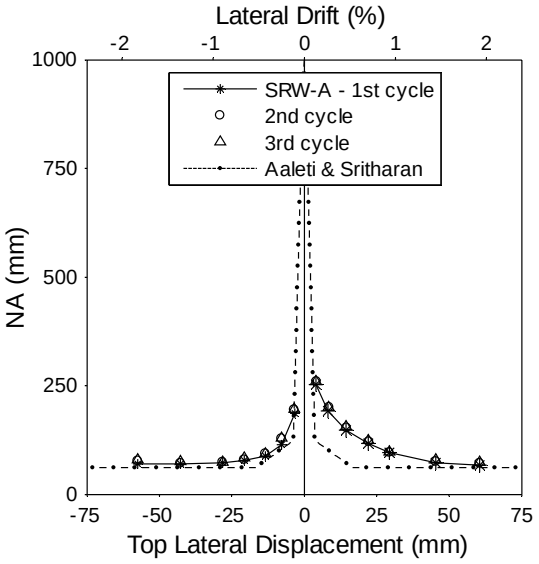

(b) SRW-A neutral axis

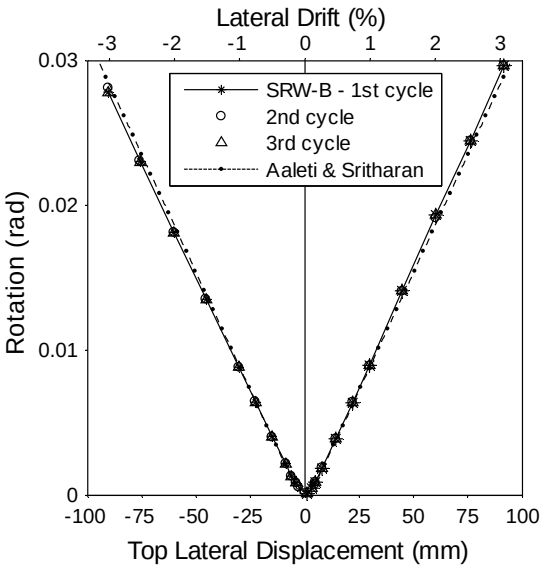

(c) SRW-B rotation

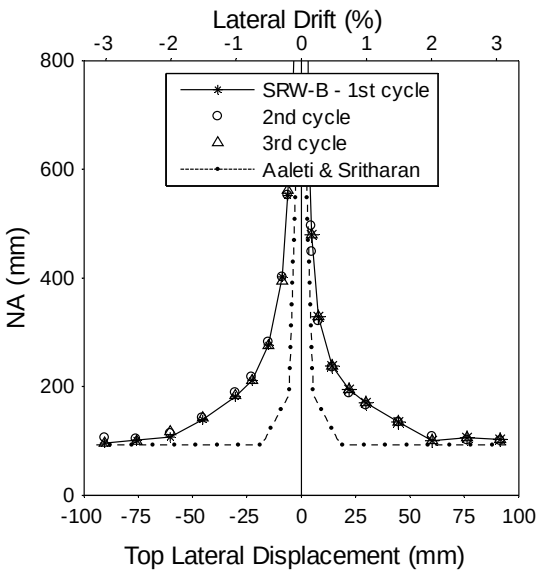

(d) SRW-B neutral axis

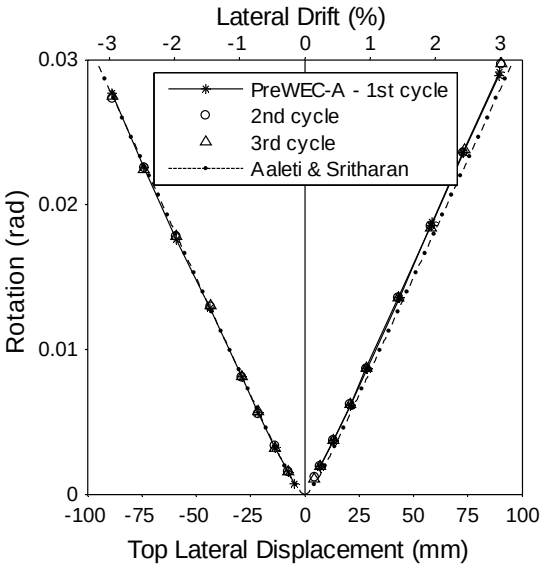

(e) PreWEC-A1 rotation

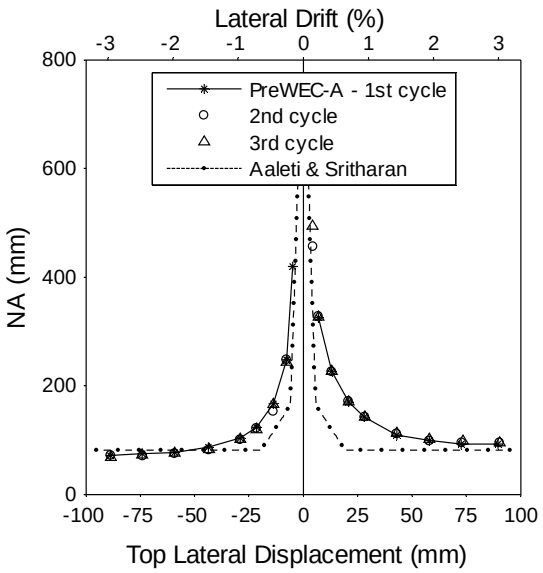

(f) PreWEC-A1 neutral axis

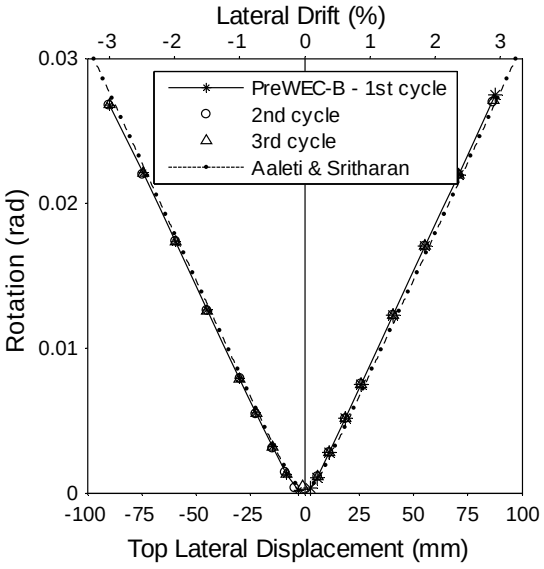

(g) PreWEC-B rotation

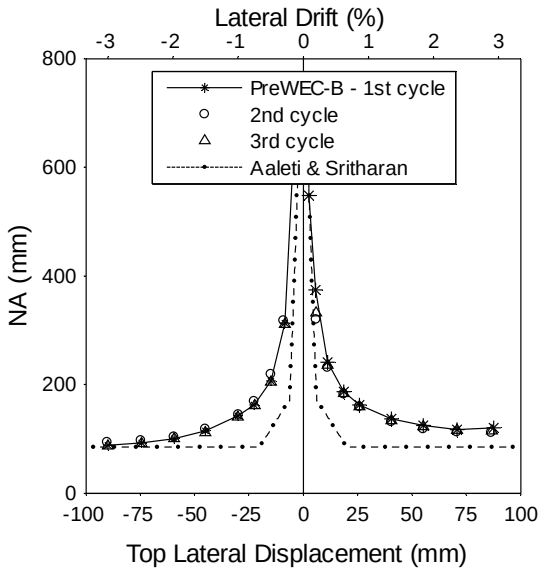

(h) PreWEC-B neutral axis

458 **Figure 15 – Change in neutral axis depth and rotation with top lateral drift**

459 **4.8 Concrete strains**

460 The compressive strains measured using both the surface and embedded strain gauges for all

461 wall tests are plotted in Figure 16. An example of the full cyclic response of the compressive

462 strain versus lateral drift of an embedded strain gauge in the east toe for PreWEC-A is
463 presented in Figure 16 (a). Since the strain gauge is located at the east toe there is an increase
464 in compressive strain with increasing positive lateral displacement. The observed constant
465 strain in the negative displacement direction represents the irrecoverable residual strain. The
466 PreWEC-A2 test wall had already undergone the A1 test and therefore initially measured the
467 total residual strain at the completion of the PreWEC-A1 test.

468 To assess the maximum strain demand clearly, the envelop peak strains in the compressive toe
469 for the first cycle to each drift level are plotted in Figure 16 (b-f) for all of the working strain
470 gauges. For SRW-A, strains in excess of 0.004 were measured by the embedded strain gauges
471 at 2% lateral drift in both directions. This measured compressive strain was reasonably
472 consistent with the maximum compressive strain of 0.0064 at 2% lateral drift calculated by
473 the simplified analysis method and used for the wall design. For SRW-B, PreWEC-A1,
474 PreWEC-A2 and PreWEC-B which used the foam strips at the toes, the maximum concrete
475 compressive strain at 3% lateral drift calculated using the simplified analysis method were
476 0.0147, 0.0128, 0.0129, and 0.0133, respectively. The measured compressive strains for these
477 walls were significantly lower than this analytical prediction ranging from 0.0025 to 0.005.
478 The measured strains were generally below concrete crushing strain of 0.003 which correlated
479 well the minimal damage observed in the wall toe and proved that the walls were well
480 designed and that the foam strip was successful in minimising compressive strains and
481 spalling of the cover concrete in the wall toe.

482 A comparison of the average measured surface strain at each wall end for the SRW-B,
483 PreWEC-A1, PreWEC-A2 and PreWEC-B tests is shown in Figure 17. These walls provided
484 a valid comparison of strains as the same dimensions were used and foam strips were used for

all four walls. The average measured surface strain for walls SRW-B, PreWEC-A1 and PreWEC-B were similar in amplitude and followed a consistent trend with increasing lateral drift. Thus the compressive strain in the wall toe strains were independent of whether the system was SRW-B or PreWEC-A or B, further confirming that the wall axial force was independent of the number of O-connectors.

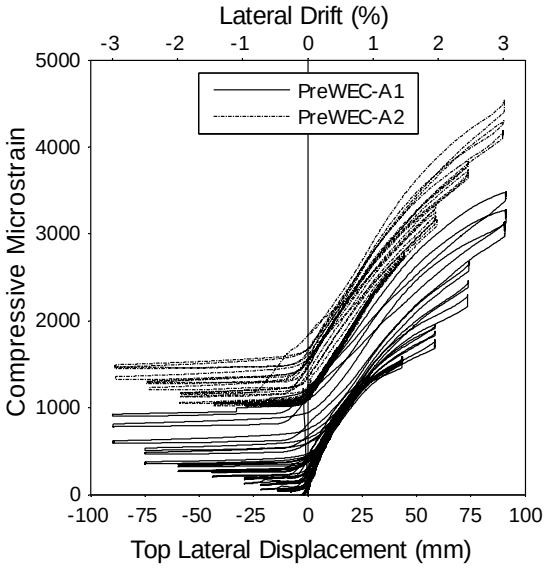

(a) PreWEC-A Embedded strain gauge (East)

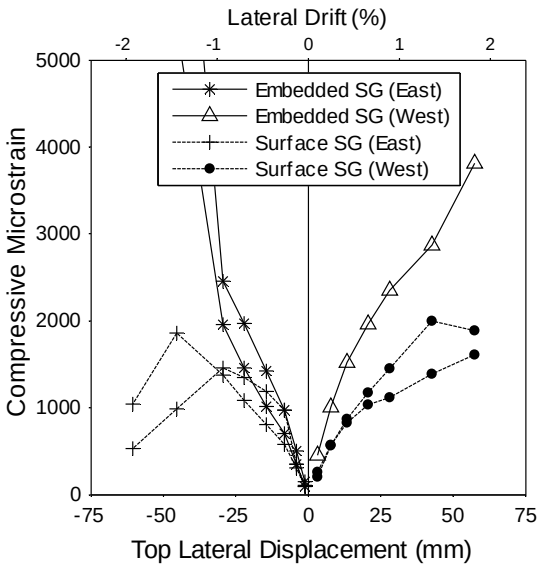

(b) SRW-A

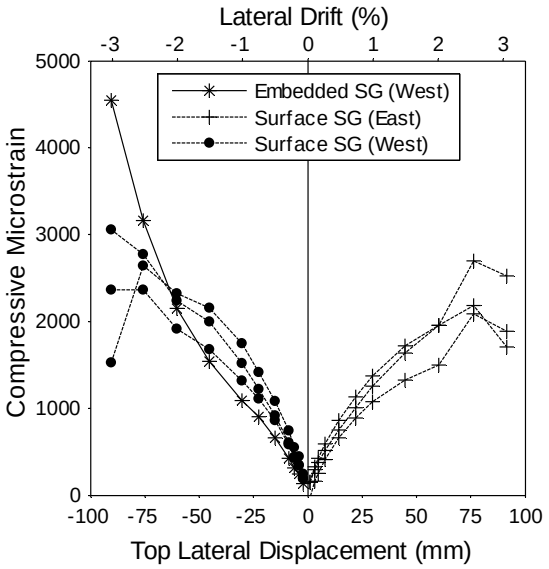

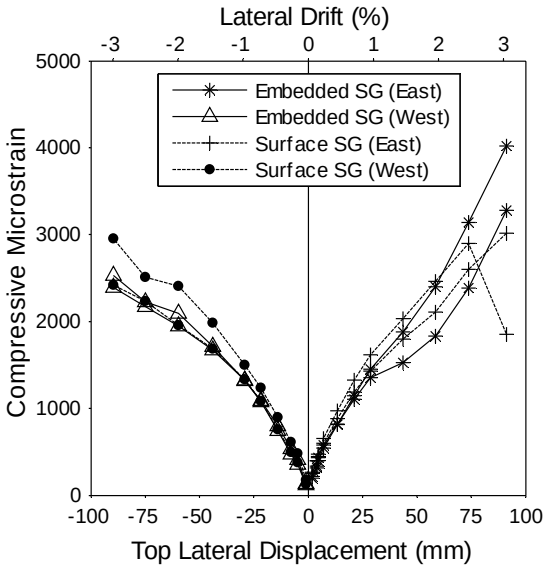

(c) SRW-B

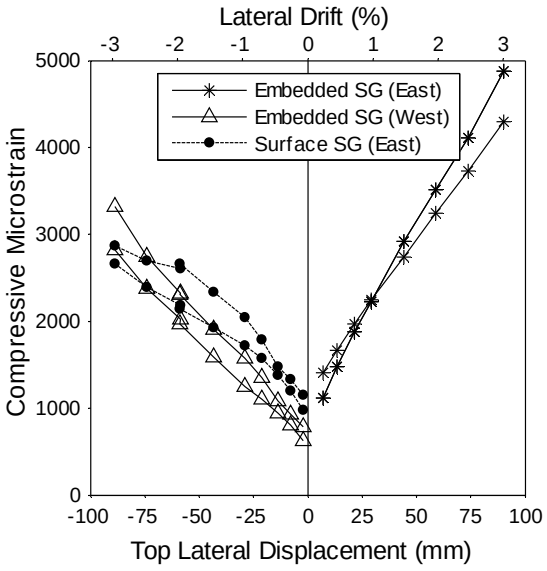

(d) PreWEC-A1

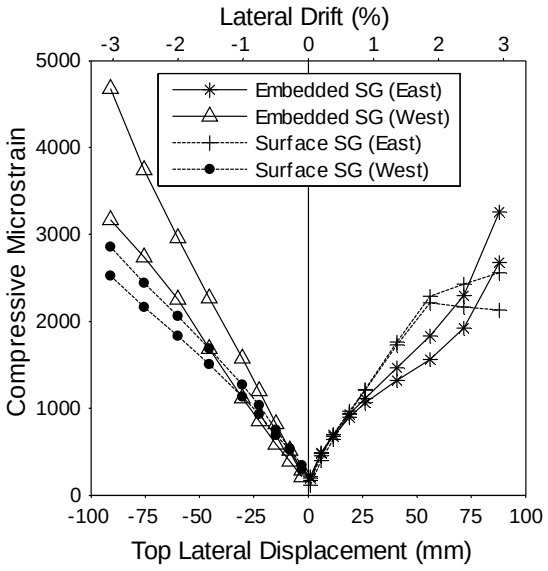

(e) PreWEC-A2

(f) PreWEC-B

490 **Figure 16 – Measured strain versus lateral drift**

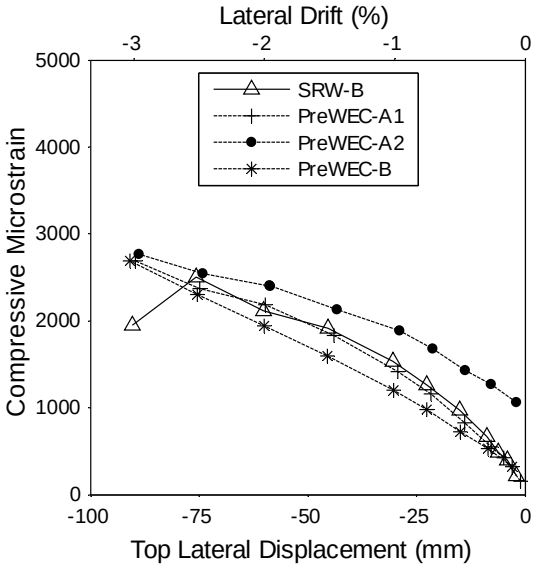

(a) West wall end

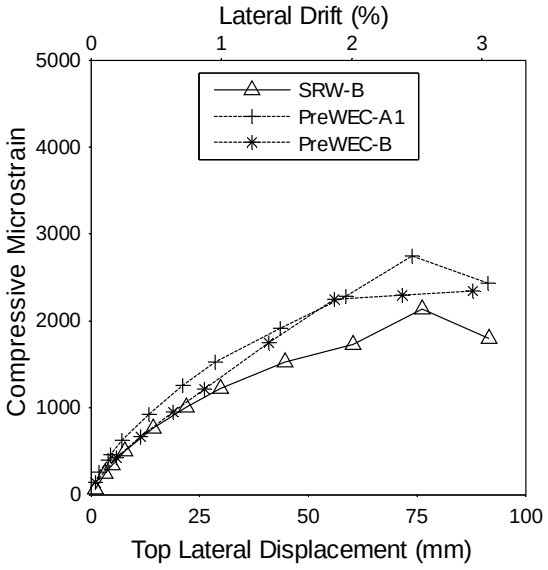

(b) East wall end

491 **Figure 17 – Average measured strain versus lateral drift**

5 INFLUENCE OF O-CONNECTORS

The PreWEC system was designed so that the O-connectors would yield in both directions of loading as both uplift and compression occurred at the ends of the wall. By undergoing a full cyclic hysteresis the O-connectors can dissipate significant energy and improve the seismic performance of the PreWEC system. The relative vertical displacement imposed on the O-connector measured during the PreWEC tests confirmed that the O-connectors yield at both ends of the wall. Because the inelastic strength of the O-connector in both the positive and negative loading directions is similar, the connectors impose equal and opposite forces on the wall panel and the axial load on the wall is not significantly affected by the number of connectors. This mechanism was confirmed by the similarities in the observed wall behaviour, damage, and measured neutral axis depth and compressive strains for SRW-B, PreWEC-A and PreWEC-B which had consistent dimensions and PT arrangement. The fact that the wall behaviour is independent of the number of O-connectors in the PreWEC system offers a significant advantage over other wall systems as supplemental damping can be added without compromising the wall design or performance.

As O-connectors were added in the PreWEC system, a significant increase in the hysteretic energy dissipation was observed from SRW-B to PreWEC-A and PreWEC-B. This increase in energy dissipation would have substantial benefits when considering the seismic performance, but did lead to an increase in residual drifts of the overall wall system. Because the concrete compressive strains and neutral axis depth were the same for SRW-B, PreWEC-A1 and PreWEC-B, the increase in measured residual drift between the SRW and PreWEC systems was primarily attributed to the increased hysteresis area provided by the O-connectors. However, it should be noted that the residual drifts observed during the PreWEC

tests are not an issue if the requirements for self-centring are considered appropriately during the design process using procedures previously developed [21].

6 CONCLUSIONS

An experimental program consisting of five cyclic tests on four unbonded PT precast concrete wall systems was conducted including two SRW (SRW-A and SRW-B) and two PreWEC systems (PreWEC-A and PreWEC-B). This experimental study systematically investigated the cyclic response of specimens with varying amounts of energy dissipation while keeping constant the initial post-tensioning, wall dimensions and confinement details for three walls and altering them significantly for the fourth wall. This allowed comparison of a variety of wall behaviours against a previously developed simplified analysis method. For all tests the walls generally behaved as expected with only minor damage occurring at large lateral drifts. Based on the test observations and the measured results, the following conclusions were drawn:

- All of the four test walls were well designed with sufficient confinement and armouring details. Selection of an axial force ratio less than 10% led to an efficient design with a reduced risk of crushing in the wall toe. The use of the foam strip below the wall toe in SRW-B, PreWEC-A and PreWEC-B helped to further reduce the compressive strains and prevent the cover concrete spalling.

- Both SRW-A and SRW-B exhibited an approximate bi-linear response with a small amount of hysteresis equal to 3-5 % EVD. The increase in EVD of SRW-B compared to SRW-A from 3% to 5% at 2% lateral drift demonstrated the influence of axial force ratio and inelastic strain in the wall toe on the hysteretic damping in the system.

- PreWEC-A and PreWEC-B showed increased strength and hysteresis due to the addition of the O-connectors. The EVD increased in proportion to the number of O-connectors with between 1.1-1.4% EVD provided by each O-connector in the PreWEC walls tested.

- The PreWEC arrangement results in connector forces imposed on the wall panel that are equal and opposite. As a result of these balanced connector forces, the wall panel behaviour is independent of the number of O-connectors and so supplemental damping can be added without compromising the wall design or performance.

- The increase in hysteresis area from an increase in O-connector number introduced higher residual drifts during the tests that need to be considered when designing the wall system to self-centre.

- The simplified analytical method published by Aaleti and Sritharan [23] was able to capture both the global and local response parameters of all tests with sufficient accuracy. There were some small discrepancies in the prediction of the neutral axis depth at low lateral drifts and the deviation between the measured and predicted PT tendon force was due to minor prestress losses observed during each test.

- The initial stiffness of the walls was lower than the expected stiffness calculated using the gross section moment of inertia. An effective stiffness modifier was calculated based on the measured initial stiffness and the predicted initial stiffness. The proportion of the gross second moment of inertia required for the effective initial stiffness to be equal to the measured initial stiffness was between 0.61-0.64Ig for SRW specimens and 0.77-0.79Ig for PreWEC specimens.

7 ACKNOWLEDGEMENTS

Funding for this research was provided by the University of Auckland Engineering Faculty Research and Development Fund. Support is also provided by National Science Foundation research award no. 1041650 through collaboration with Iowa State University. Materials were donated by Stresscrete Northern Ltd, Contech, and Sika New Zealand. Assistance provided by Alex Shegay, James King, Dan Ripley, and Mark Byrami was much appreciated. Opinions, findings, conclusions, and recommendations in this paper are those of the authors, and do not necessarily represent those of the sponsors.

8 REFERENCES

[1] Kam WY, Pampanin S, Elwood K. Seismic performance of reinforced concrete buildings in the 22 February Christchurch (Lyttelton) earthquake. Bulletin of the New Zealand Society for Earthquake Engineering. 2011;44:239-78.

[2] Sritharan S, Beyer K, Henry RS, Chai YH, Kowalsky M, Bull D. Understanding Poor Seismic Performance of Concrete Walls and Design Implications. Earthquake Spectra. 2014;30:307-34.

[3] Priestley MJN, Sritharan SS, Conley JR, Pampanin S. Preliminary results and conclusions from the PRESSS five-story precast concrete test building. PCI Journal. 1999;44:42-67.

[4] Erkmen B, Schultz AE. Self-centering behavior of unbonded, post-tensioned precast concrete shear walls. Journal of Earthquake Engineering. 2009;13:1047-64.

[5] Stavridis A, Koutromanos I, Shing PB. Shake-table tests of a three-story reinforced concrete frame with masonry infill walls. Earthquake Engineering and Structural Dynamics. 2012;41:1089-108.

[6] Henry RS, Brooke NJ, Sritharan S, Ingham JM. Defining concrete compressive strain in unbonded post-tensioned walls. ACI Structural Journal. 2012;109:101-12.

[7] Holden T, Restrepo J, Mander JB. Seismic performance of precast reinforced and prestressed concrete walls. Journal of Structural Engineering. 2003;129:286-96.

[8] Restrepo JI, Rahman A. Seismic performance of self-centering structural walls incorporating energy dissipators. Journal of Structural Engineering. 2007;133:1560-70.

[9] Smith BJ, Kurama YC, McGinnis MJ. Design and measured behavior of a hybrid precast concrete wall specimen for seismic regions. Journal of Structural Engineering. 2011;137:1052-62.

[10] Smith BJ, Kurama YC. Seismic design guidelines for solid and perforated hybrid precast concrete shear walls. PCI Journal. 2014;59:43-59.

[11] Smith BJ, Kurama YC. Seismic displacement demands for hybrid precast concrete shear walls. Structures Congress 2013: Bridging Your Passion with Your Profession - Proceedings of the 2013 Structures Congress. 2013.

[12] Marriott D. The Development of High-Performance Post-Tensioned Rocking Systems for the Seismic Design of Structures [PhD Thesis]. Christchurch: University of Canterbury; 2009.

[13] Kurama YC. Seismic design of unbonded post-tensioned precast concrete walls with supplemental viscous damping. ACI Structural Journal. 2000;97:648-58.

[14] Kurama YC. Simplified seismic design approach for friction-damped unbonded post-tensioned precast concrete walls. ACI Structural Journal. 2001;98:705-16.

[15] Kurama YC. Hybrid post-tensioned precast concrete walls for use in seismic regions. PCI Journal. 2002;47:36-59.

[16] Sritharan S, Aaleti S, Henry RS, Liu KY, Tsai KC. Introduction to PreWEC and key results of a proof of concept test. Pavia, Italy: IUSS Press; 2008.

[17] Henry RS, Aaleti S, Sritharan S, Ingham JM. Concept and finite-element modeling of new steel shear connectors for self-centering wall Systems. Journal of Engineering Mechanics. 2010;136:220-9.

[18] Twigden KM. Dynamic response of unbonded post-tensioned rocking walls [PhD Thesis]. Auckland: The University of Auckland; 2015.

[19] New Zealand Standard. Concrete Structures Standard NZS 3101. Wellington, New Zealand 2006.

[20] Sritharan S, Aaleti S, Thomas DJ. Seismic analysis and design of precast concrete jointed wall systems. ISU-ERI-Ames Report ERI-07404. Ames, IA: Department of Civil, Construction and Environmental Engineering, Iowa State University; 2007.

[21] Henry RS. Self-centering precast concrete walls for buildings in regions with low to high seismicity [PhD Thesis]: University of Auckland; 2011.

[22] Mander JB, Priestley MJN, Park R. Theoretical stress-strain model for confined concrete. Journal of structural engineering New York, NY. 1988;114:1804-26.

[23] Aaleti S, Sritharan S. A simplified analysis method for characterizing unbonded post-tensioned precast wall systems. Engineering Structures. 2009;31:2966-75.

[24] Henry RS, Sritharan S, Ingham JM. Recentering requirements for the seismic deisgn of self-centering systems. Proceedings of the Ninth Pacific Conference on Earthquake Engineering. 2011. Auckland, New Zealand

[25] Henry RS, Aaleti S, Sritharan S, Ingham JM. Seismic analysis of a low-damage PREcast Wall with End Columns (PreWEC) including interaction with floor diaphragms. SESOC Journal. 2012;25.

[26] Oyarzo-Vera CA, McVerry GH, Ingham JM. Seismic zonation and default suite of ground-motion records for time-history analysis in the North Island of New Zealand. Earthquake Spectra. 2012;28:667-88.

[27] Standards Association of Australia. Metallic materials : tensile testing at ambient temperature. 4th ed. ed. Sydney, NSW: Sydney, NSW : Standards Australia 2007.; 2007.

[28] Walsh KQ, Kurama YC. Behavior and design of anchorages for unbonded post-tensioning strands in seismic regions. 2008 Structures Congress - Structures Congress 2008: Crossing the Borders. 2008. Vancouver, BC

[29] ACI Innovation Task Group 5. Acceptance criteria for special unbonded post-tensioned precast structural walls based on validation testing and commentary : an ACI standard. Farmington Hills, Mich.: American Concrete Institute; 2008.

[30] Aaleti S, Henry RS, Liu KY, Sritharan S, Tsai KC. Experimental investigation of a precast wall with end columns (PreWEC) system. Eleventh East Asia-Pacific Conference on Structural Engineering & Construction (EASEC-11) "Building a Sustainable Environment". 2008. Taipei, Taiwan

[31] Chopra AK. Dynamics of structures : Theory and applications to earthquake engineering. 3rd ed. Upper Saddle River, NJ: Prentice Hall; 2007.